Title: Elephant megacarcasses increase local nutrient pools in African savanna soils and plants

Courtney G. Reed[1*], Michelle L. Budny[2], Johan T. du Toit[3,4], Ryan Helcoski[3], Joshua P. Schimel[1], Izak P. J. Smit[5,6], Tercia Strydom[5], Aimee Tallian[3,7], Dave I. Thompson[8,9], Helga van Coller[8,10], Nathan P. Lemoine[2,11], Deron E. Burkepile[1,8*]

[1]Department of Ecology, Evolution, and Marine Biology, University of California, Santa Barbara, CA, USA

[2]Department of Biological Sciences, Marquette University, Milwaukee, WI, USA

[3]Department of Wildland Resources, Utah State University, Logan, UT, USA

[4]Institute of Zoology, Zoological Society of London, London, England, UK

[5]Scientific Services, South African National Parks, Skukuza, South Africa

[6]Sustainability Research Unit, Nelson Mandela University, George, South Africa

[7]Norwegian Institute for Nature Research, Høgskoleringen 9 Trondheim, 7485 Norway

[8]South African Environmental Observation Network (SAEON), Ndlovu Node, Phalaborwa, South Africa

[9]Unit for Environmental Sciences and Management, Potchefstroom Campus, North West University, Potchefstroom, South Africa

[10]The Expanded Freshwater and Terrestrial Environmental Observation Network (EFTEON), Kimberley 8306, South Africa

[11]Department of Zoology, Milwaukee Public Museum, Milwaukee, WI, USA

23 *Corresponding authors: Courtney Reed, courtneyreed@ucsb.edu, Deron Burkepile,

24 dburkepile@ucsb.edu

Abstract

African elephants (*Loxodonta africana*) are the largest extant terrestrial mammals, with bodies containing enormous quantities of nutrients. Yet we know little about how these nutrients move through the ecosystem after an elephant dies. Here, we investigated the initial effects (1-26 months postmortem) of elephant megacarcasses on savanna soil and plant nutrient pools in Kruger National Park, South Africa. We hypothesized that: (H1) elephant megacarcass decomposition would release nutrients into soil, resulting in higher concentrations of soil nitrogen (N), phosphorus (P), and micronutrients near the center of carcass sites; (H2) carbon (C) inputs to the soil would stimulate microbial activity, resulting in increased soil respiration potential near the center of carcass sites; and (H3) carcass-derived nutrients would be absorbed by plants, resulting in higher foliar nutrient concentrations near the center of carcass sites. To test our hypotheses, we identified 10 elephant carcass sites split evenly between nutrient-poor granitic and nutrient-rich basaltic soils. At each site, we ran transects in the four cardinal directions from the center of the carcass site, collecting soil and grass (*Urochloa trichopus,* formerly *U. mosambicensis*) samples at 0, 2.5, 5, 10, and 15 m. We then analyzed samples for CNP and micronutrient concentrations and quantified soil microbial respiration potential. We found that concentrations of soil nitrate, ammonium, $\delta^{15}N$, phosphate, and sodium were elevated closer to the center of carcass sites (H1). Microbial respiration potentials were positively correlated with soil organic C, and both respiration and organic C decreased with distance from the carcass (H2). Finally, we found evidence that plants were readily absorbing carcass-derived nutrients from the soil, with foliar %N, $\delta^{15}N$, iron, potassium, magnesium, and sodium significantly elevated closer to the center of carcass sites (H3). Together, these results indicate that elephant megacarcasses release ecologically consequential pulses of nutrients into the soil

48 that influence soil microbial activity and are absorbed by plants into the above-ground nutrient
49 pools. These localized nutrient pulses may drive spatiotemporal heterogeneity in plant diversity,
50 herbivore behavior, and ecosystem processes.

Sect. 1 Introduction

Living animals affect nutrient flows through ecosystems (Schmitz et al. 2018), but we have only recently acknowledged that the nutrients from animal carcasses could also influence ecosystem processes (Barton et al. 2013; Monk et al. 2024). In marine ecosystems, whale carcasses function as unique hotspots of nutrient cycling, biodiversity, and ecosystem processes (Roman et al. 2014). In terrestrial systems, mass mortality events (e.g., wildebeest, cicadas) create nutrient hotspots (Yang, 2004; Subalusky et al. 2020), while individual small and medium-sized carcasses release pulses of nutrients into the soil (Town, 2000; Barton et al. 2016; Olea et al. 2019). Yet, terrestrial ecosystem ecology lacks knowledge about the role of megacarcasses (carcasses of animals such as elephants and rhinoceros that are >1000 kg at death) as potential drivers of spatiotemporal heterogeneity in nutrient cycling and ecosystem processes. Importantly, these megacarcasses may be functionally different than smaller carcasses due to the extraordinarily high concentration of nutrients and residence time of the decomposing animal (see reviews by Barton et al. 2013; Barton, 2016; Barton & Bump 2019). This question around the role of megacarcasses is particularly relevant given the megaherbivore losses that occurred during the Pleistocene extinctions and that are still occurring today (Ripple et al. 2015). We are only beginning to understand how the 'extinction aftershock' of losing the largest species impacts ecosystems (Owen-Smith, 1989; Flannery, 1990), and no study has yet investigated how the loss of megacarcasses might influence the dynamics of terrestrial ecosystems (Doughty et al. 2013; Doughty et al. 2016).

We can only evaluate the importance of terrestrial megacarcasses for nutrient cycling in ecosystems where megaherbivores still exist, such as African savannas. The African savanna elephant (*Loxodonta africana*) is the largest extant land animal and is known for its key

ecological effects in savannas while alive (e.g., dispersing seeds, creating plant refuges, preventing woody encroachment) (Skarpe et al. 2004; Asner et al. 2009; Campos-Arceiz & Blake, 2011; Coverdale et al. 2016; Guy et al. 2021). Yet, the elephant's large body mass may mean that it also has an outsized impact in these ecosystems even after death. A 4000-kg elephant megacarcass likely represents ~2000 kg carbon (C), ~300 kg nitrogen (N), and ~125 kg phosphorus (P) deposited in the savanna landscape (estimated from stoichiometry of elephants and other mammals in Sterner & Elser, 2002). The N deposition from one elephant megacarcass (in a 700 m^2 impact zone assuming a 15 m disturbance radius) is roughly equivalent to the N delivered to 10,000 m^2 of savanna from ~100 years from atmospheric deposition (Mphepya et al. 2006).

If megacarcasses provide large nutrient pulses, then they likely create hotspots of important below- and aboveground processes. Belowground, soil respiration and organic matter decomposition might increase with nutrient inputs from carcasses (Risch et al. 2020). Concentrations of C, N, P, and potassium (K) are often elevated near carcasses of medium-sized animals (e.g., bison, moose, kangaroo, vicuña) (Towne, 2000; Bump et al. 2009a; Macdonald et al. 2014; Risch et al. 2020; Monk et al. 2024), and nutrients such as P and calcium (Ca) continue leaching from bones even after soft tissues have been consumed or degraded (Coe, 1978; Keenan & Beeler, 2023). Aboveground, plant growth in African savannas is limited by nutrient availability, most commonly N and P (Ries & Shugart, 2008; Pellegrini, 2016), and micronutrients such as sodium (Na) and potassium (K) may co-limit plant productivity as well (Epron et al. 2012; Chen et al. 2024). Thus, the large influx of nutrients released from megacarcasses might increase the mobilization of nutrients by plants, potentially increasing nutrient accessibility for vertebrate and invertebrate herbivores (Yang, 2008; Grant & Scholes,

2006; Anderson et al. 2010; Joern et al. 2012). Indeed, carcasses of smaller vertebrates (e.g., salmon, deer) can increase the proportions of nitrogen and $\delta^{15}N$ (an indicator of animal-driven N) in plants within just a few months postmortem (Hocking & Reynolds, 2012; van Klink et al. 2020).

To assess the effects of megacarcasses on local nutrient pools (Figure 1), we measured the initial contributions of elephant carcasses (1-26 months postmortem) to soil and plant nutrients in the Kruger National Park (KNP), South Africa. Further, we examined the effects of elephant carcasses on the two main soil types in KNP: sandy, relatively nutrient-poor granitic soils and clayey, relatively nutrient-rich basaltic soils (Venter et al. 2003). At each site, we ran transects in each cardinal direction from the center of the site where an elephant died, collecting samples of soil and a palatable grass species (*Urochloa trichopus*) at 0, 2.5, 5, 10, and 15 m. We then analyzed soil samples for CNP and micronutrient content, quantified soil microbial respiration potential, and measured %N, $\delta^{15}N$, and macro- and micronutrient content in grass tissue. We hypothesized that: (H1) elephant megacarcass decomposition would release nutrients into soil, resulting in higher concentrations of soil N, P, and micronutrients near the center of carcass sites; (H2) C inputs to the soil would stimulate microbial activity, resulting in increased soil respiration potential near the center of carcass sites; and (H3) carcass-derived nutrients would move from soil into plants, resulting in higher foliar nutrient concentrations near the center of carcass sites. We predicted that enrichment effects from megacarcasses would be greater on sites with fresher carcasses relative to older carcasses and on nutrient-poor granitic sites compared to nutrient-rich basaltic sites.

Sect. 2 Methods

2.1 Study system and sample collection

We performed this research in the southern part of the Kruger National Park (KNP), South Africa (24.996 S, 31.592 E, ~275m elevation). The two dominant soil types in KNP are granitic soils (Inceptisols) and basaltic soils (Versitols or Andisols) (Khomo et al. 2017). The clay-rich basaltic soils have relatively large surface area, enabling them to retain larger quantities of water than granitic soils, which drain water more quickly and therefore are lower in water-soluble nutrients (Buitenweref, Kulmatiski, & Higgins, 2014; Rughöft et al. 2016). The landscape of KNP is a mix of savanna grasslands and broadleaf woodlands, with an overstory dominated by trees from the genus *Combretum* (red bushwillow, *C. apiculatum*; russet bushwillow, *C. hereroense*; leadwood, *C. imberbe*) and trees formerly known as acacias (knobthorn, *Senegalensis nigrescens*; umbrella thorn, *Vachellia tortillis*). The park hosts a full suite of African savanna animals, including ~30,000 elephants (*Loxodonta africana*) (Coetsee & Ferreira, 2023), with a mortality rate of ~2% (~600 elephants per year). The targeted region of KNP has a high density of scavengers and predators, including white-backed vultures (*Gyps africanus*), spotted hyenas (*Crocuta crocuta*), and lions (*Panthera leo*) (Owen-Smith & Mills, 2007).

During the wet season in March 2023, we identified ten elephant carcass sites (1-26 months postmortem), five on relatively nutrient-rich basaltic soil and five on nutrient-poor granitic soil. KNP section rangers provided precise GPS locations of where elephant carcasses had been found. Most elephants died of old age, illness, injury, or, in the case of one young bull, fighting over territory. Carcass sites were recognizable *in situ* by a persistent bonefield, undigested gut contents, and an absence of herbaceous vegetation. At each site, we hammered a rebar post into the center of the megacarcass disturbance and ran 15 m transects out from the

post in each of the four cardinal directions. We collected green leaf material from *U. trichopus,* a common and abundant palatable grass species, and used an auger to collect soil samples to a depth of 10 cm at five points along each transect (0.5, 2.5, 5, 10, and 15 m) (Bump, Peterson, & Vucetich, 2009; Holdo & Mack, 2014; Gray & Bond, 2015; Monk et al. 2024). We treated the 10-15m distances as representative of background concentrations of nutrients based on pilot data showing that the effect of elephant carcasses on soil nutrient concentrations was undetectable at this distance away from the carcass site, similar to studies on the carcasses of other large vertebrates (e.g., Towne, 2000; Bump et al. 2009). We pooled and homogenized the samples to yield one composite leaf and one composite soil sample per sampling distance from each carcass site. Soil samples were sieved in a 5-mm metal sieve which was cleaned in between samples with 70% ethanol. Soil samples were stored in a cooler during fieldwork. On the day they were collected, we used 5 g of each soil sample for soil respiration measurements (described below). The rest of each sample was placed in a plastic bag on the day of collection and stored in a -20°C freezer for up to 1 month; samples were stored in coolers with ice blocks during the transition from the freezer at the field site to the lab for analysis. We chose to freeze samples rather than storing at room temperature based on literature demonstrating that the impacts of freezing on soil nitrate and ammonium concentrations are fairly minimal, except in specific cases of high soil acidity or peaty soils that were not present at our field site (Esala, 1995; Turner & Romero, 2009; Sollen-Norrlin & Rintoul-Hynes, 2024). Leaf samples were stored in paper bags at room temperature until dried for analyses (see below).

2.3 Hypothesis testing

We tested our first hypothesis that elephant carcass decomposition would release nutrients into the soil by performing soil nutrient analyses. We sent 250 g of each soil sample to Eco-Analytica laboratory at the North-West University in Potchefstroom, South Africa for measurements of soil concentrations of ammonium $[NH_4]^+$, nitrate $[NO_3]^-$, phosphate $[PO_4]^{3-}$, and plant-available P. Samples were air-dried and sieved through < 2mm mesh prior to chemical analysis. Plant-available P was extracted from 4 g of soil and 30 ml extraction fluid (1:7.5 ratio) using an acid–fluoride solution (P Bray-1) (FAO, 2021), measured colorimetrically using a Systea EasyChem200 analyser, and expressed as mg/kg. The detection limit was 0.5 mg/kg, and plant available P measurements <0.5 mg/kg were replaced with half the detection limit (0.25 mg/kg) (Croghan & Egeghy, 2003). Water-soluble nitrate and phosphate anions were extracted from volume on volume 100 mg soil and 200 ml deionized water (Sonneveld & van den Ende, 1981), analyzed by ion chromatography on a Metrohm 930 Compact Flex System, and measured as mg/L. Ammonium (also 1:2 water extract) was analyzed colorimetrically using a Systea EasyChem200 analyzer and measured as mg/L. Detection limits for soil ions were 0.01 mg/L, and soil ion concentrations measured as <0.01 mg/L were replaced with half the detection limit (0.005 mg/L). To convert the nitrate, ammonium, and phosphate units from mg/L to mg/kg, we multiplied by 2, based on the 1:2 soil to water extraction ratio.

To determine whether soil micronutrients were distinct and elevated at the center of carcass sites relative to soil further from the center, we measured concentrations of sodium (Na), magnesium (Mg), iron (Fe), calcium (Ca), potassium (K), and phosphorus (P). Air-dried and sieved (>2 mm) soil samples, weighed to 0.2 g, were microwaved in 9 ml 65% nitric acid (HNO_3) and 3 ml 32% hydrochloric acid (HCl) according to EPA 3051b in a Milestone, Ethos microwave digester with UP, Maxi 44 rotor. A period of 20 minutes allowed the system to reach

188 1800 MW at a temperature of 200 °C which was maintained for 15 minutes. After cooling, the
189 samples were brought up to a final volume of 50 ml and analyzed on an Agilent 7500 CE ICP-
190 MS fitted with CRC (Collision Reaction Cell) technology for interference removal. The
191 instrument is optimized using a solution containing Li, Y, Ce, and Tl (1 ppb) for standard low-
192 oxide/low interference levels (≤ 1.5%) while maintaining high sensitivity across the mass range.
193 The instrument was calibrated using ULTRASPEC® certified custom mixed multi-element stock
194 standard solutions containing all the elements of interest (De Bruyn Spectroscopic Solutions,
195 South Africa). Calibrations spanned the range of 0 – 30 ppm for the mineral elements Ca, Mg,
196 Na, and K and 0 – 0.3 ppm for the rest of the trace elements. Elemental concentrations were
197 expressed as mg/kg.
198 Finally, to determine whether elevated N levels in soils were derived from the carcass, we
199 sent 10 g of each sample to the BIOGRIP laboratory within the Central Analytical Facility at
200 Stellenbosch University for measurements of soil %N and $\delta^{15}N$, obtained using a Vario Isotope
201 Select Elemental Analyzer connected to a thermal conductivity detector and an Isoprime
202 precisions isotope ratio mass spectrometer (IRMS). Samples were oven-dried at 60°C for 48
203 hours and milled to a fine powder using a Retsch MM400 mill (Germany). The powdered
204 samples were weighed (2 – 60 mg) prior to combustion at 950°C. The gasses were reduced to N_2
205 (undiluted) in the reduction column, which was held at 600°C. A high organic carbon (HOC) soil
206 standard (0.52 ± 0.02 %N), along with two international reference standards (USGS40 ($\delta^{15}N$ -
207 4.52% AIR) and USGS41 ($\delta^{15}N$ +47.57% AIR)) were used for calibration. The N elemental
208 content was expressed relative to atmospheric N as N_2 δ^{15}NAIR (‰). The quantification limit for
209 $\delta^{15}N$ on the IRMS is 1 nA (nanoAmp), and the quantification limit for %N is 0.06%. The

210 precision for %N was 0.02% and for $\delta^{15}N$ is ±0.11%, determined using the HOC standard, which
211 was run multiple times throughout the analysis.
212 To test our second hypothesis that nutrient inputs to the soil would stimulate microbial
213 activity, we measured soil organic C, water content, and microbial respiration potential. We sent
214 10 g of each sample to the BIOGRIP laboratory for measurements of soil organic C using a
215 Vario TOC Cube (Elementar, Germany). Samples (dried and milled as above) were weighed (10
216 – 60 mg), acidified using 10% HCl to remove the total inorganic C (carbonates), and dried
217 overnight at 60°C. All samples were analyzed through combustion at 950°C. The released CO_2
218 was measured by a non-dispersive infrared (NDIR) sensor. A high organic C (7.45 ± 0.14 %C)
219 soil standard from Elemental Microanalysis Ltd (UK) was included during the analysis. The
220 quantification limit for %C is 0.14%. The precision for the %C was 0.09% and was determined
221 using the low organic C (LOC) standard (1.86 ± 0.14 %C), which was run multiple times
222 throughout the analysis.
223 To quantify soil respiration and water content, we used an incubation method (Lemoine
224 et al. 2023) in which 5 g (± 0.2 g) of each sample was placed into a 100 ml clear glass bottle,
225 sealed, and flushed with CO_2-free air. Following flushing, we incubated the bottles for one hour
226 at 25°C. We then recorded CO_2 concentrations using an LI-850 CO_2/H_2O infrared gas analyzer.
227 After soil respiration measurements, we determined sample dry weight by drying each sample at
228 60°C for 24-48 hours until stable mass was achieved. We subtracted dry weight from starting
229 weight to obtain soil water content. Finally, we used the dry weights and the Ideal Gas Law to
230 standardize all respiration measurements to CO_2 $\mu g\ h^{-1} g\ dry\ soil^{-1}$.
231 To test our third hypothesis that carcass-derived nutrients would be incorporated by
232 plants, we measured foliar nutrient concentrations in *U. trichopus*. Two grams of each dried leaf

sample was sent to the BIOGRIP laboratory for preparation and measurements of %N and $\delta^{15}N$ via stable isotope analysis as described above. A Sorghum flour standard (1.47 ± 0.25 %N) from Elemental Microanalysis Ltd (UK) was used for calibration, along with two international reference standards (USGS40 and USGS41). The quantification limit for $\delta^{15}N$ on the IRMS is 1 nA, and the quantification limit for %N is 1.3%. The precision for the %N was 0.02% and for $\delta^{15}N$ is ±0.08‰. Limits were determined using the sorghum flour standard, which was run multiple times throughout the analysis. Additionally, we sent 5 g per sample to Cedara Analytical Services Laboratory to quantify micronutrients in grass tissue (P, Na, Mg, K, Ca, and Fe) using Inductively Coupled Plasma Optical Emission Spectroscopy (ICP-OES 5800, Agilent, USA). Samples were dried (110°C overnight) and milled to a fine powder. Subsamples (0.5 g) were ashed at 450°C for 4 hours, and the ash was re-wet using 2 mL conc. HCl (32%). Samples were evaporated to dryness then re-suspended in 25 mL 1M HCl before filtering. Lastly, the filtrate was diluted with de-ionized water in a ratio of 5:20 filtrate to water. To calibrate the ICP-OES, solutions containing known amounts of each element were measured (10-20 ppm for Na and C, 200-1500 ppm for Fe, 0.5-3.75% for K, and 0.125-0.5% for P), prepared from 1000 ppm primary single standards. At three of the ten sites, we did not find sufficient plant material at the central point for analysis, resulting in a sample size of N = 7 for the center (distance = 0.5m) measurement for leaf nutrient analyses.

To test whether each response variable for the three hypotheses was significantly associated with soil type and/or distance from the carcass center, we performed a model selection procedure. For each response variable, we ran five generalized linear mixed models using the gamma family (link = log) in the package *lme4* (Bates et al. 2015): (*i*) soil type + distance + soil type × distance interaction, (*ii*) soil type + distance, (*iii*) soil type, (*iv*) distance, and (v) a null

256 model indicating no significant difference in slope or intercept after accounting for carcass site.
257 All models included carcass site as a random effect to account for individual variation. Each
258 model included 50 observations (10 sites x 5 distances per site). For samples in which the
259 nutrient level was listed as 0 or undetectable, we accounted for the uncertainty by using half the
260 detection level as described above. The narrow distribution of ages (1-26 months since death)
261 with the sample size of N = 10 sites made testing for the effect of age challenging, so we did not
262 include carcass age in the models. We compared the models for each response variable using
263 Akaike Information Criterion (AICc). Models with a ΔAICc ≤ 2 were considered roughly
264 equivalent in fit (Burnham and Anderson, 2002).
265 In addition to these models, for our second hypothesis we regressed soil respiration
266 potential against soil organic C, expecting that the two would be positively correlated. We ran a
267 generalized linear mixed model with soil respiration potential as the response variable. The
268 model included soil organic C + distance + soil type, with carcass site as a random effect. We did
269 not include an interaction with soil type in this model due to sample size restrictions. Respiration
270 potential and organic C were both log-transformed to achieve normality.
271 To determine whether leaf and soil micronutrient composition differed with distance and
272 soil type, we ran permutational analysis of variance (perMANOVA) in *vegan* (Oksanen et al.
273 2022). We ran the same model separately for soil and leaf micronutrient composition (soil type +
274 distance). To determine which micronutrients contributed most to compositional differences
275 across distances and soil types, we calculated samplewise Bray-Curtis dissimilarity and
276 performed principal component analysis. We also tested for differences in variance in
277 micronutrient composition across distances and soil types using “betadisper” in *vegan* (Oksanen

et al. 2022). We ran linear models to test for correlations between leaf and soil concentrations of each micronutrient. Each model included distance as a covariate and site as a random effect.

Finally, to test the impact of carcass age on key soil metrics, we ran exponential decay functions for soil ammonium, nitrate, phosphate, and respiration verses carcass age for samples from the center of the carcass site (0.5m sampling location). We also performed a t-test to verify that there was no difference in mean carcass age across soil types.

All statistical analyses were performed in R version 4.2.1 (R Core Team, 2022).

Sect. 3 Results

3.1 Hypothesis 1: Effects of megacarcasses on soil nutrient pools

We found partial support for our first hypothesis that soil N and P concentrations would be higher closer to the center of carcass sites (Table S1). Soil %N (Figure 2A) was overall greater in basaltic soils, and it decreased with distance from the carcass site on granitic soils. Soil nitrate (Figure 2B) decreased with distance from the carcass site but did not differ between soil types. Ammonium (Figure 2C) also decreased with distance, but only in granitic soils. $\delta^{15}N$ (Figure 2D) was greater in granitic soils and decreased with distance in both soil types, indicating that the proportion of animal-sourced N in the soil was greater near the center of the carcass site. Soil phosphate, plant available P, and mineral P (Figure 2E-G) all exhibited significant soil × distance interactions. Phosphate (Figure 2E) was highly elevated at the center of carcass sites and decreased steeply with distance, but only in granitic soils. Plant-available P (Figure 2F) decreased with distance in both soil types, but the effect was strongest in granitic soils. Finally, mineral P (Figure 2G) was greater in basaltic soils, and there was a small decrease with distance in granitic soils but not in basaltic soils.

Contrary to our first hypothesis, soil micronutrient composition did not differ significantly with distance from the carcass center; nor did most individual micronutrients (Table S1). The perMANOVA results showed that soil micronutrient composition did not differ significantly with distance ($R^2 = 0.00$, $F_{4,44} = 0.0$, $P = 1.000$) (Figure S2A), but it did differ significantly with soil type ($R^2 = 0.71$, $F_{1,44} = 108.8$, $P = 0.001$) (Figure S2B). There was no significant difference in variance with distance ($F_{4,45} = 0.0$, $P = 0.996$) or soil type ($F_{1,48} = 2.6$, $P = 0.115$). Principal components analysis showed that dimension 1 explained 53.6% of the variation between soil types and was driven primarily by differences in Mg, Ca, and Fe. Dimension 2 explained 25.9% of variation and was driven primarily by differences in K. Soil Na (Figure S3A) was marginally greater in granitic soils and decreased with distance from the carcass, with the effect greater in granitic soils. Soil K (Figure S3B) was greater in basaltic soils and decreased marginally with distance. Soil Fe, Mg, and Ca (Figure S3C-E) were greater in basaltic soils, with minimal effects of distance.

3.2 Hypothesis 2: Effects of megacarcasses on soil carbon and respiration

Consistent with our second hypothesis, soil respiration potential was marginally positively correlated with soil organic carbon concentration and decreased significantly with distance but did not differ with soil type (Figure 3). We found no evidence for differences in soil water content (Figure S4A) or soil pH (Figure S4B) with distance or soil type. In both cases, the null ranked among the set of top models (Table S1).

3.3 Hypothesis 3: Effects of megacarcasses on plant nutrient pools

Consistent with our third hypothesis, we found elevated foliar nutrient concentrations in *U. trichopus* at elephant carcass sites. Leaf %N (Figure 4A) and $\delta^{15}N$ (Figure 4B) both decreased with distance from the carcass center. $\delta^{15}N$ exhibited a significant soil × distance interaction in which it was overall greater in basaltic soils, but the difference between the two soil types was greater closer to the carcass site. Foliar P was greater in basaltic soils and decreased only marginally with distance in the granite soils. Finally, the foliar N:P ratio was greater in granitic soils and decreased with distance in the basaltic soils.

Leaf micronutrient composition did not differ significantly with distance ($R^2 = 0.13$, $F_{4,40} = 1.9$, $P = 0.062$; Figure S5A) but did differ with soil type ($R^2 = 0.17$, $F_{1,40} = 9.7$, $P = 0.001$; Figure S5B). There was no significant difference in variance with distance ($F_{4,41} = 0.5$, $P = 0.713$) or soil type ($F_{1,44} = 1.9$, $P = 0.173$). Dimension 1 explained 42.8% of the variance across soil types and was primarily driven by Mg, Na, and P. Dimension 2 explained 26.6% of the variance and was driven mainly by K, Ca, and Fe. Foliar Na (Figure S6A) and Mg (Figure S6B) were both greater in basaltic soils and decreased with distance from the carcass center. Foliar K (Figure S6C) and Fe (Figure S6D) both decreased with distance as well but did not differ with soil type. The null model was in the top set for foliar Ca, indicating no significant relationship between foliar Ca concentrations and soil type or distance from the carcass center. Individual micronutrients (K, Ca, Mg, Fe) were not correlated between leaf and soil samples, with the exception of Na (Table S3).

3.4 Effects of carcass age on soil ions and respiration potential

Soil ammonium ($\alpha = 0.018$, $P < 0.001$), phosphate ($\alpha = 0.023$, $P < 0.001$), and respiration potential ($\alpha = 0.058$, $P < 0.001$) all decreased significantly with carcass age (Figure 5A-C). The

346 exponential decay model for nitrate failed to converge due to an outlier with extremely high soil
347 nitrate (1454 mg/kg) at 258 days postmortem (Figure 5D). We ran a t-test to test for a difference
348 in mean carcass age between soil types and found no significant difference between the two
349 groups ($P = 0.294$).
350
351 **Sect. 4 Discussion**
352 Here, we show that elephant megacarcasses influence soil and foliar nutrients during at least the
353 first two years following mortality. Consistent with our hypotheses, soil nitrate (Figure 2B),
354 ammonium (Figure 2C), $\delta^{15}N$ (Figure 2D), and P (Figure 2E-F) concentrations were all elevated
355 at the center of carcass sites and decreased with distance from the center. Soil %N, nitrate,
356 ammonium, and plant-available P concentrations at the 15m point were consistent with those
357 found in other studies of soil nutrient content in Kruger (Aranibar et al. 2003; Rughöft et al.
358 2016), confirming that the 15m point serves as an effective baseline control in this experiment.
359 Microbial respiration potential was also elevated towards the center of carcass sites and was
360 correlated with the abundance of organic C (Figure 3). Finally, %N (Figure 4A) and $\delta^{15}N$ in a
361 common grass (Figure 4B) were both elevated closer to the centers of carcass sites compared to
362 grass farther from carcasses. Together, these results indicate that carcass-derived nutrients move
363 into soil and subsequently get absorbed by plants over relatively short time scales, cycling
364 essential nutrients such as N from carrion into the soil and then back into aboveground nutrient
365 pools.
366 The initial influx of ammonium from elephant carcasses may have time-dependent
367 impacts on plant abundance at elephant carcass sites. The mean ammonium level at the center of
368 carcass sites (34.8 mg/kg) was higher than the level generally considered toxic to plants (Britto

& Kronzucker, 2002). Yet, we found living grass—typically *U. trichopus*—in the center of the carcass site at seven out of ten of our sites (ammonium range 10-172 mg/kg) and at the 2.5m distance for all sites (ammonium range 0-72 mg/kg). The three sites without vegetation in the center had the highest ammonium levels (70-144 mg/kg), suggesting that *U. trichopus* has a higher degree of ammonium tolerance than some sympatric grass species but may still be limited by the high ammonium levels at the centers of these three relatively fresh carcass sites. However, the recentness of the disturbance from the carcass likely also plays a role in determining plant abundance near the center of the carcass. Because of the elephant carcass site age distribution, (mean 350 days postmortem; range 24-811 days), this study may not have captured the full impact of ammonium release from carcasses during the early stages of decomposition. Soil ammonium spiked early and decreased rapidly (Figure 5A), and future research on carcasses within the first few weeks postmortem would enhance our understanding of these early nutrient dynamics.

Soil nitrate (Figure 2B) and soil respiration potential (Figure 3) were also elevated near the center of carcass sites, indicating higher activity rates for nitrifying bacteria and heterotrophic microbes (Prosser, 2011). These results are consistent with other work on carrion, where microbial activity tends to be greater in soils near carcasses as compared to surrounding soil (Bump et al. 2009b). However, carcass effects on soil microbial respiration exhibit a high degree of intra-system variation (Risch et al. 2020), and the potentially short window during which increased respiration occurs may make capturing these variations challenging. For example, soil respiration potential at the center of the three youngest carcass sites was on average 2x higher than the seven older sites (18.43 and 9.62 μg CO_2 per hour per gram of dry soil, respectively; Figure 5D). Thus, the impact of increased organic C on soil microbial processes may be

relatively short lived and only last a matter of months (Keenan et al. 2018; Keenan, Schaeffer, & DeBruyn, 2019). These trends are consistent with soil ammonium and phosphate, both of which are highest at the youngest carcass sites (<200 days postmortem; Figure 5A-B). Soil microbial respiration rate is also highly elevated early on, but it decreases at a faster rate over time than soil ions (Figure 5C). Thus, soil dynamics during the first several months after death may play a crucial role in determining the long-term impacts of megacarcasses on savannas and therefore provides a promising avenue for future research.

Elevated soil phosphate (Figure 2E) and plant-available P (Figure 2F) at the center of carcass sites were also consistent with expectations from the literature (Bump et al. 2009a; Parmenter & MacMahon, 2009). However, elevated P levels in soil did not translate to elevated P in grass leaves (Figure 4C), which could suggest a lag between trends in soil and plants that is longer for P than for N. This lag could occur because phosphate easily forms chemical bonds with other soil ions (e.g., iron and aluminum in acidic soils and calcium in basic soils). Nitrate does not form these bonds and therefore has greater water solubility and mobility in soils and may be more readily taken up by plants (Wiersum, 1962; Arai & Sparks, 2007). However, it is also possible that P limitation in Kruger is not as strong as it is in some other African savanna systems (Pellegrini, 2016). The foliar N:P ratios measured in this experiment were higher closer to the center of the carcass site (median 9.38 at 0 m and 4.83 at 15 m), indicating that N limitation may be relatively stronger further from the carcass site, and P limitation may be relatively stronger closer to the center (Figure 4D, Table S2). These relatively high foliar N:P ratios at the center of carcass sites are similar to those found in N fertilization studies in Kruger (Craine et al. 2008), further supporting the idea that the influx of N from megacarcasses may shift the soil from relatively more N limited to more P limited.

The elevated plant-available P at the center of carcass sites likely came primarily from phosphate released from decomposing tissue (Yong et al. 2019). Bone decomposition, which is also likely a major source of P from animal carcasses (Subalusky et al. 2020), occurs over long time scales (Coe, 1978; Subalusky et al. 2020) and therefore should result in the slow release of P and a gradual decrease in the N:P ratio (Parmenter & MacMahon, 2009; Quaggiotto et al. 2019). Indeed, initial inorganic N influxes to the Mara River in Kenya from mass wildebeest die-offs are 10-fold greater than concurrent increases in P, which instead releases slowly over about seven years of bone decomposition (Subalusky et al. 2017). Research following megacarcasses over longer timeframes postmortem is needed to clarify when P from enriched soil is absorbed by plants and at what stage megacarcass bones begin contributing to soil P dynamics. It is also possible that bone dispersal by scavengers may result in less P leaching from bones close to where the elephant died and more P being distributed across the landscape at distances far from the carcass site.

The contributions of megacarcasses to soil nutrient pools were strongly associated with soil type. Our results confirmed the previously-established trend that basaltic soils are overall more cation rich than granitic soils, with greater concentrations of P, K, Fe, Mg, and Ca (Figure 2G; Figure S3B-E; Gertenbach, 1983; Craine, Morrow, & Stock, 2008; Wigley et al. 2014). However, soil ammonium, $\delta^{15}N$, and phosphate were all higher in the granitic soils towards the center of carcass sites, decreasing steeply to be similar to basaltic soils about 10 m from the carcass center (Figure 2C-E). These results indicate that the impact of organic matter from megacarcasses may be stronger in relatively nutrient-poor and sandy granitic soil compared with nutrient-rich and clayey basaltic soil. We were surprised that grass on basaltic soil did not consistently exhibit greater nutrient concentrations. One potential explanation is that grass may

438 primarily be limited by macronutrients like N and P on both soil types (Craine et al. 2008;
439 Holdo, 2013) rather than by micronutrients. Thus, even with increased micronutrient availability
440 their actual uptake may not differ substantially. Studies on ungulate carcasses (e.g., muskoxen,
441 moose, zebra) have shown increased foliar N at carcass sites (Danell et al. 2002; Bump et al.
442 2009b; Turner et al. 2014), but to date there is little research on the flow of micronutrients from
443 carrion to plants and none on the pipeline from megacarcasses to plants. Moreover, it remains to
444 be seen whether increases in foliar N and other nutrients affect herbivory rates at carcass sites
445 and how long such effects may last.

446 The magnitude of nitrogen inputs from megacarcasses, as well as the substantial size and
447 duration of their impact zones, means their impacts on ecosystem processes may be functionally
448 distinct from smaller carrion. Soil nitrate concentrations at elephant carcass sites are orders of
449 magnitude higher than at carcass sites of smaller carrion (e.g., rabbits, white-tailed deer,
450 kangaroo) (Quaggiato et al. 2019; Bump et al. 2009; Barton et al. 2016). Even for large ungulates
451 such as moose, total soil inorganic nitrogen (ammonium + nitrate) at carcass sites is a mean 300
452 mg/kg (Bump, Peterson, & Vucetich, 2009), substantially lower than the mean total soil
453 inorganic nitrogen at elephant carcass sites (2.5m distance; 473 mg/kg). Termite mounds,
454 another long-lasting source of savanna nutrient heterogeneity, have mean soil nitrate
455 concentrations (197 mg/kg) lower than elephant carcass sites, but maximum nitrate
456 concentrations that are on par with them (974 mg/kg) (Seymour et al. 2014), again indicating that
457 elephant carcasses are one of the strongest known individual contributors of soil nitrogen in
458 African savanna ecosystems, which may have important implications for savanna ecology.
459 Indeed, there is evidence that carcass size strongly impacts scavenger food web structure
460 (Moleón et al. 2015; Morris et al. 2023). Moreover, the attraction of animals to carcasses via

461 scavenging, predation, or mourning (Goldenberg & Wittemyer, 2020) could have positive
462 feedbacks on nutrient cycling (Bump, Peterson, & Vucetich, 2009; Monk et al. 2024), which
463 may be magnified by carcass size. Thus, the impacts of megacarcasses on savanna ecosystem
464 processes may be dissimilar to the effects of small carrion and more similar to other more
465 persistent contributors to savanna ecosystem processes, such as termite mounds (Davies et al.
466 2016), cattle bomas (Augustine, 2003), and even mass animal mortality events (Subalusky et al.
467 2017, 2020).
468
469 **Sect. 5 Conclusions**
470 This study is an important first step in understanding the ecological legacies of megacarcasses on
471 savanna ecosystem processes. During the first two years postmortem, elephant carcasses released
472 pulses of nitrogen and phosphate, which influence savanna primary productivity. These nutrients
473 stimulated soil microbial activity and enriched foliar N, and the effects were strongest in
474 nutrient-poor soil, with potential long-term impacts on savanna nutrient heterogeneity. These
475 carcass-derived nutrient hotspots represent a previously unstudied function of megaherbivores on
476 savannas—one that we need to better understand in order to comprehend the full impacts of
477 megaherbivore population declines in modern ecosystems.
478
479 **Data and Code Availability:** Data and computer code are archived on Dryad Digital Repository
480 (https://doi.org/10.5061/dryad.wpzgmsbwm).
481
482 **Author Contributions:** Deron E. Burkepile, Nathan P. Lemoine, Izak P. J. Smit, Tercia
483 Strydom, Aimee Tallian, Johan T. du Toit, Dave I. Thompson, and Joshua P. Schimel conceived
484 the study. Michelle L. Budny, Johan T. du Toit, Nathan P. Lemoine, Joshua P. Schimel, Izak P.

J. Smit, Tercia Strydom, Aimee Tallian, Dave I. Thompson, Helga van Coller, and Deron E. Burkepile collected samples. Courtney G. Reed, Nathan P. Lemoine, Dave I. Thompson, and Deron E. Burkepile analyzed the data. Courtney G. Reed drafted the manuscript, and all authors contributed to editing.

Competing Interests: The authors declare that they have no conflict of interest.

Acknowledgments: Funding for this research was provided by the National Science Foundation (#s 2128092, 2128093, and 2128094) and the University of California Santa Barbara Academic Senate. All research was completed under permits from South African National Parks (SS554). We thank the field assistants of SANParks for guiding and protection in the field, as well as the section rangers and Sandra Snelling for GPS locations and ages of carcasses. We thank Mr. Lucky Sithole (Cedara Analytical Services Laboratory), Ms. Terina Vermeulen (Eco-Analytica Laboratory), and Dr. Janine Colling (BIOGRIP laboratory) for extensive laboratory support. Select data used in this research paper were generated using equipment in the DSI funded BIOGRIP soil and water node at Stellenbosch University.

References

1. Agbenin, J. O. & Yakubu, S. Potassium-calcium and potatssium-magnesium exchange equilibria in an acid savanna soil from northern Nigeria. *Geoderma*, 136, 542-554, https://doi.org/10.1016/j.geoderma.2006.04.008, 2006.

2. Anderson, T. M., Hopcraft, J. G. C., Eby, S., Ritchie, M., Grace, J. B., & Olff, H. Landscape-scale analyses suggest both nutrient and antipredator advantages to Serengeti herbivore hotspots. *Ecol.,* 91, 1519–1529, https://doi.org/10.1890/09-0739.1, 2010.
3. Aranibar, J. N., Macko, S. A., Anderson, I. C., Potgieter, A. L. F., Sowry, R. & Shugart, H. H. Nutrient cycling responses to fire frequency in the Kruger National Park (South Africa) as indicated by stable isotope analysis. *Isotopes Environ. Health Stud.,* 39, 141-158, https://doi.org/10.1080/1025601031000096736, 2003.
4. Aria, Y. & Sparks, D. L. Phosphate reaction dynamics in soils and soil components: a multiscale approach. *Adv. Agron*., 94, 135-179, https://doi.org/10.1016/S0065-2113(06)94003-6, 2007.
5. Asner, G. P., Levick, S. R., Kennedy-Bowdoin, T., Knapp, D. E., Emerson, R., Jacobson, J., Colgan, M. S., & Martin, R. E. Large-scale impacts of herbivores on the structural diversity of African savannas. *PNAS*, 106, 4947–4952, https://doi.org/10.1073/pnas.0810637106, 2009.
6. Augustine, D. J. Long-term, livestock-mediated redistribution of nitrogen and phosphorus in an East African savanna. *J. Appl. Ecol*., 40, 137-149, https://doi.org/10.1046/j.1365-2664.2003.00778.x, 2003.
7. Barton, P. S., Cunningham, S. A., Lindenmayer, D. B., & Manning, A. D. The role of carrion in maintaining biodiversity and ecological processes in terrestrial ecosystems. *Oecologia*, 171, 761–772, https://doi.org/10.1007/s00442-012-2460-3, 2013.
8. Barton, P.S. Carrion Ecology, Evolution, and Their Applications. Edited by: M.E. Benbow, J.K. Tomberlin, A.M. Tarone. CRC Press, Boca Raton, FL, USA. 2016.

9. Barton, P. S., McIntyre, S., Evans, M. J., Bump, J. K., Cunningham, S. A., & Manning, A. D. Substantial long-term effects of carcass addition on soil and plants in a grassy eucalypt woodland. *Ecosphere,* 7, e01537, https://doi.org/10.1002/ecs2.1537, 2016.
10. Barton, P.S., Bump, J.K. Carrion decomposition. In: Carrion Ecology and Management. Edited by: P.P. Olea, P. Mateo-Tomas, J.A. Sanchez-Zapata. Springer, NY, USA, 101-124, 2019.
11. Bates, D., Mächler, M., Bolker, B., & Walker, S. Fitting linear mixed-effects models using lme4. *J. Stat. Softw*., 67, 1–48, https://doi.org/10.18637/jss.v067.i01, 2015.
12. Britto, D. T., & Kronzucker, H. J. NH_4^+ toxicity in higher plants: a critical review. *J. Plant Physiol.,* 159, 567–584, https://doi.org/10.1078/0176-1617-0774, 2002.
13. Buitenwerf, R., Kulmatiski, A. & Higgins, S. I. Soil water retention curves for the major soil types of the Kruger National Park. *Koedoe*, 56, a1228, http://dx.doi.org/10.4102/koedoe.v56i1.1228, 2014.
14. Bump, J. K., Peterson, R. O., & Vucetich, J. A. Wolves modulate soil nutrient heterogeneity and foliar nitrogen by configuring the distribution of ungulate carcasses. *Ecol.,* 90, 3159–3167, https://doi.org/10.1890/09-0292.1, 2009.
15. Bump, J. K., Webster, C. R., Vucetich, J. A., Peterson, R. O., Shields, J. M., & Powers, M. D. (2009). Ungulate carcasses perforate ecological filters and create biogeochemical hotspots in forest herbaceous layers allowing trees a competitive advantage. *Ecosyst.,* 12, 996–1007, https://doi.org/10.1007/s10021-009-9274-0, 2009.
16. Burnham, K. P. & Anderson, D. R. Model Selection and Multimodel Inference. Springer New York, NY. http://doi.org/10.1007/b97636, 2002.

17. Campos-Arceiz, A., & Blake, S. Megagardeners of the forest – the role of elephants in seed dispersal. *Acta Oecol*., 37, 542–553, https://doi.org/10.1016/j.actao.2011.01.014, 2011.
18. Chen, J., Gutjahr, C., Bleckmann, A., & Dresselhaus, T. Calcium signaling during reproduction and biotrophic fungal interactions in plants. *Mol. Plant,* 8, 595–611, https://doi.org/10.1016/j.molp.2015.01.023, 2015.
19. Chen, B., Fang, J., Piao, S., Ciais, P., Black, T. A., Wang, F., Niu, S., Zeng, Z. & Luo, Y. A meta-analysis highlights globally widespread potassium limitation in terrestrial ecosystems. *New Phytologist,* 241, 154-165, https://doi.org/10.1111/nph.19294, 2024.
20. Coe, M. The decomposition of elephant carcasses in the Tsavo (East) National Park, Kenya. *J. Arid Environ.,* 1, 71–86, https://doi.org/10.1016/S0140-1963(18)31756-7, 1978.
21. Coetsee, M. & Ferreira, S. Bridging science, management, and opinion: GLTFCA elephant management [Conference presentation]. Savanna Science Network Meeting, Skukuza, Kruger National Park, South Africa, 2023 March 5-9.
22. Coverdale, T. C., Kartzinel, T. R., Grabowski, K. L., Shriver, R. K., Hassan, A. A., Goheen, J. R., Palmer, T. M., & Pringle, R. M. Elephants in the understory: opposing direct and indirect effects of consumption and ecosystem engineering by megaherbivores. *Ecol.,* 97, 3219–3230, https://doi.org/10.1002/ecy.1557, 2016.
23. Craine, J. M., Morrow, C., & Stock, W. D. Nutrient concentration ratios and co-limitation in South African grasslands. *New Phytol.,* 179, 829–836, https://doi.org/10.1111/j.1469-8137.2008.02513.x, 2008.
24. Croghan C. & Egeghy P. P., Methods of dealing with values below the limit of detection using SAS. *Southern SAS User Group,* 22, 2003.

572 25. Danell, K., Berteaux, D., & Bråthen, K. A. Effect of muskox carcasses on nitrogen
573 concentration in tundra vegetation. *Arctic*, 55, 389–392, http://www.jstor.org/stable/40512497,
574 2002.
575 26. Davies, A. B., Levick, S. R., Robertson, M. P., van Rensburg, B. J., Asner, G. P. & Parr, C.
576 L. Termite mounds differ in their importance for herbivores across savanna types, seasons
577 and spatial scales. *Oikos*, 125, 726-734, https://doi.org/10.1111/oik.02742, 2016.
578 27. Doughty, C. E., Roman, J., Faurby, S., Wolf, A., Haque, A., Bakker, E. S., Malhi, Y.,
579 Dunning, J. B., Jr, & Svenning, J.-C. Global nutrient transport in a world of giants. *PNAS,*
580 113, 868–873, https://doi.org/10.1073/pnas.1502549112, 2016.
581 28. Doughty, C. E., Wolf, A., & Malhi, Y. The legacy of the Pleistocene megafauna extinctions
582 on nutrient availability in Amazonia. *Nat. Geosci.,* 6, 761–764,
583 https://doi.org/10.1038/ngeo1895, 2013.
584 29. Epron, D., Laclau, J-P., Almeida, J. C. R., Gonçalves, J. L. M., Ponton, S., Sette, Jr., C. R.,
585 Delgado-Rojas, J. S., Bouillet, J-P. & Nouvellon, Y. Do changes in carbon allocation account
586 for the growth response to potassium and sodium applications in tropical Eucalyptus
587 plantations? *Tree Physiology*, 32, 667-679, https://doi.org/10.1093/treephys/tpr107, 2012.
588 30. Esala, M. J. Changes in the extractable ammonium- and nitrate-nitrogen contents of soil
589 samples during freezing and thawing. *Commun. Soil Sci. Plant Anal*., 26, 61-68,
590 https://doi.org/10.1080/00103629509369280, 1995.
591 31. FAO. Standard operating procedure for soil available phosphorus - Bray I and Bray II
592 method. http://www.fao.org/3/cb3460en/cb3460en.pdf, 2021.

32. Flannery, T. F. Pleistocene faunal loss: implications of the aftershock for Australia's past and future. *Archaeol. Ocean*., 25, 45–55, https://doi.org/10.1002/j.1834-4453.1990.tb00232.x, 1990.

33. Gertenbach, W. Landscapes of the Kruger National Park. *Koedoe*, 26, 9-121, https://doi.org/10.4102/koedoe.v26i1.591, 1983.

34. Goldenberg, S. Z. & Wittemyer, G. Elephant behavior toward the dead: A review and insights from field observations. *Primates,* 61, 119-128, https://doi.org/10.1007/s10329-019-00766-5, 2020.

35. Grant, C. C., & Scholes, M. C. The importance of nutrient hot-spots in the conservation and management of large wild mammalian herbivores in semi-arid savannas. *Biol. Conserv.,* 130, 426–437, https://doi.org/10.1016/j.biocon.2006.01.004, 2006.

36. Gray, E. F. & Bond, W. Soil nutrients in an African forest/savanna mosaic: Drivers or driven? *S. Afr. J. Bot.,* 101, 66-72, https://doi.org/10.1016/j.sajb.2015.06.003, 2015.

37. Guy, T. J., Hutchinson, M. C., Baldock, K. C. R., Kayser, E., Baiser, B., Staniczenko, P. P. A., Goheen, J. R., Pringle, R. M., & Palmer, T. M. Large herbivores transform plant-pollinator networks in an African savanna. *Curr. Biol.,* 2964–2971, https://doi.org/10.1016/j.cub.2021.04.051, 2021.

38. Hocking, M. D. & Reynolds, J. D. Nitrogen uptake by plants subsidized by Pacific salmon carcasses: a hierarchical experiment. *Can. J. For. Res.,* 42, 908-917, https://doi.org/10.1139/x2012-045, 2012.

39. Holdo, R. M. Effects of fire history and N and P fertilization on seedling biomass, specific leaf area, and root:shoot ratios in a South African savannah. *S. Afr. J. Bot*., 86, 5–8, https://doi.org/10.1016/j.sajb.2013.01.005, 2013.

40. Holdo, R. M. & Mack, M. C. Functional attributes of savanna soils: contrasting effects of tree canopies and herbivores on bulk density, nutrients and moisture dynamics. *J. Ecol.,* 102, 1171-1182, https://doi.org/10.1111/1365-2745.12290, 2014.

41. Hu, L., Wu, Z., Robert, C. A. M., Ouyang, X., Züst, T., Mestrot, A., Xu, J., & Erb, M. Soil chemistry determines whether defensive plant secondary metabolites promote or suppress herbivore growth. *PNAS*, 118, e2109602118, https://doi.org/10.1073/pnas.2109602118, 2021.

42. Joern, A., Provin, T., & Behmer, S. T. Not just the usual suspects: insect herbivore populations and communities are associated with multiple plant nutrients. *Ecol.,* 93, 1002–1015, https://doi.org/10.1890/11-1142.1, 2012.

43. Kaspari, M. The invisible hand of the periodic table: how micronutrients shape ecology. *Annu. Rev. Ecol. Evol. Syst.,* 52, 199–219, https://doi.org/10.1146/annurev-ecolsys-012021-090118, 2021.

44. Keenan, S. W., Schaeffer, S. M., Jin, V. L. & DeBruyn, J. M. Mortality hotspots: nitrogen cycling in forest soils during vertebrate decomposition. *Soil Biol. Biochem.,* 121, 165-176, https://doi.org/10.1016/j.soilbio.2018.03.005, 2018.

45. Keenan, S. W., Schaeffer, S. M., and DeBruyn, J. M. Spatial changes in soil stable isotopic composition in response to carrion decomposition. *Biogeosciences,* 16, 3929–3939, https://doi.org/10.5194/bg-16-3929-2019, 2019.

46. Keenan, S. W., & Beeler, S. R. Long-term effects of buried vertebrate carcasses on soil biogeochemistry in the Northern Great Plains. *PloS One*, 18, e0292994, https://doi.org/10.1371/journal.pone.0292994, 2023.

638 47. Khomo, L., Trumbore, S., Bern, C. R. & Chadwick, O. A. Timescales of carbon turnover in
639 soils with mixed crystalline mineralogies. *SOIL*, 3, 17-30, https://doi.org/10.5194/soil-3-17-
640 2017, 2017.
641 48. Lathwell, D. J. & Grove, T. L. Soil-plant relationships in the tropics. *Annu. Rev. Ecol. Syst*.,
642 17, 1-16, https://www.jstor.org/stable/2096986, 1986.
643 49. Lemoine, N. P., Budny, M. L., Rose, E., Lucas, J., & Marshall, C. W. Seasonal soil moisture
644 thresholds inhibit bacterial activity and decomposition during drought in a tallgrass prairie.
645 *Oikos*, 2024, e10210, https://doi.org/10.1111/oik.10201, 2023.
646 50. Macdonald, B. C. T., Farrell, M., Tuomi, S., Barton, P. S., Cunningham, S. A., & Manning,
647 A. D. Carrion decomposition causes large and lasting effects on soil amino acid and peptide
648 flux. *Soil Biol. Biochem*., 69, 132–140, https://doi.org/10.1016/j.soilbio.2013.10.042, 2014.
649 51. Moleón, M., Sánchez-Sapata, J. A., Sebastián-González, E. & Owen-Smith, N. Carcass size
650 shapes the structure and functioning of an African scavenging assemblage. *Oikos,* 124, 1391-
651 1403, https://doi.org/10.1111/oik.02222, 2015.
652 52. Monk, J. D., Donadio, E., Smith, J. A., Perrig, P. L., Middleton, A. D., & Schmitz, O. J.
653 Predation and biophysical context control long-term carcass nutrient inputs in an Andean
654 ecosystem. *Ecosyst*., 27, 346–359, https://doi.org/10.1007/s10021-023-00893-7, 2024.
655 53. Morris, A. W., Smith, I., Chakrabarti, S., Lala, F., Nyaga, S. & Bump, J. K. Eating an
656 elephant, one bite at a time: predator interactions at carrion bonanzas. *Food Webs*, 37,
657 e00304, https://doi.org/10.1016/j.fooweb.2023.e00304, 2023.
658 54. Mphepya, J. N., Galy-Lacaux, C., Lacaux, J. P., Held, G., & Pienaar, J. J. Precipitation
659 chemistry and wet deposition in Kruger National Park, South Africa. *J. Atmos. Chem*., 53,
660 169–183, https://doi.org/10.1007/s10874-005-9005-7, 2006.

55. Oksanen J, Simpson G, Blanchet F, Kindt R, Legendre P, Minchin P, O'Hara R, Solymos P, Stevens M, Szoecs E, Wagner H, Barbour M, Bedward M, Bolker B, Borcard D, Carvalho G, Chirico M, De Caceres M, Durand S, Evangelista H, FitzJohn R, Friendly M, Furneaux B, Hannigan G, Hill M, Lahti L, McGlinn D, Ouellette M, Ribeiro Cunha E, Smith T, Stier A, Ter Braak C, Weedon J. Community Ecology Package. R package version 2.6-4, https://CRAN.R-project.org/package=vegan, 2022.

56. Olea, P.P, Mateo-Tomas, P., Sanchez-Zapata, J.A. (eds.) Carrion Ecology and Management. Springer, NY, USA, 2019.

57. Owen-Smith, N. Megafaunal extinctions: the conservation message from 11,000 years B.P. *Conserv. Biol.,* 3, 405–412, https://www.jstor.org/stable/2386221, 1989.

58. Owen-Smith, N., & Mills, M. G. L. Predator-prey size relationships in an African large-mammal food web. *J. Anim. Ecol.,* 77, 173–183, https://doi.org/10.1111/j.1365-2656.2007.01314.x, 2008.

59. Pandey, N. Role of micronutrients in reproductive physiology of plants. *Plant Stress*, 4, 1-13. https://www.semanticscholar.org/paper/af9a8662b83613f6e0d5e538ed33f3add4a1d5a1, 2010.

60. Parmenter, R. R., & MacMahon, J. A. Carrion decomposition and nutrient cycling in a semiarid shrub–steppe ecosystem. *Ecol. Monogr*., 79, 637–661, https://doi.org/10.1890/08-0972.1, 2009.

61. Pellegrini, A. F. A. Nutrient limitation in tropical savannas across multiple scales and mechanisms. *Ecol*., 97, 313–324, https://doi.org/10.1890/15-0869.1, 2016.

62. Prosser, J. I. Soil Nitrifiers and Nitrification. In Nitrification. ASM Press, pp. 347-383, 2014.

63. Quaggiotto, M.-M., Evans, M. J., Higgins, A., Strong, C., & Barton, P. S. Dynamic soil nutrient and moisture changes under decomposing vertebrate carcasses. *Biogeochemistry*, 146, 71–82, https://doi.org/10.1007/s10533-019-00611-3, 2019.

64. R Core Team. R: A language and environment for statistical computing. R Foundation for Statistical Computing, Vienna, Austria. https://www.R-project.org/, 2022.

65. Ries, L. P., & Shugart, H. H. Nutrient limitations on understory grass productivity and carbon assimilation in an African woodland savanna. *J. Arid Environ*., 72, 1423–1430, https://doi.org/10.1016/j.jaridenv.2008.02.013, 2008.

66. Ripple, W. J., Newsome, T. M., Wolf, C., Dirzo, R., Everatt, K. T., Galetti, M., Hayward, M. W., Kerley, G. I. H., Levi, T., Lindsey, P. A., Macdonald, D. W., Malhi, Y., Painter, L. E., Sandom, C. J., Terborgh, J., & Van Valkenburgh, B. Collapse of the world's largest herbivores. *Sci. Adv.,* 1, e1400103, https://doi.org/10.1126/sciadv.1400103, 2015.

67. Risch, A. C., Frossard, A., Schütz, M., Frey, B., Morris, A. W., & Bump, J. K. Effects of elk and bison carcasses on soil microbial communities and ecosystem functions in Yellowstone, USA. *Funct. Ecol.,* 34, 1933–1944, https://doi.org/10.1111/1365-2435.13611, 2020.

68. Roman, J., Estes, J. A., Morissette, L., Smith, C., Costa, D., McCarthy, J., Nation, J. B., Nicol, S., Pershing, A., & Smetacek, V. *Whales as marine ecosystem engineers. Front. Ecol. Environ.,* 12, 377–385, https://doi.org/10.1890/130220, 2014.

69. Rughöft, S., Hermann, M., Lazar, C. S., Cesarz, S., Levick, S. R., Trumbore, S. E. & Küsel, K. Community composition and abundance of bacterial, archaeal and nitrifying populations in savanna soils on contrasting bedrock material in Kruger National Park, South Africa. *Front. Microbiol.,* 7, https://doi.org/10.3389/fmicb.2016.01638, 2016.

70. Sardans, J., & Peñuelas, J. Potassium control of plant functions: ecological and agricultural implications. *Plants*, 10, https://doi.org/10.3390/plants10020419, 2021.

71. Schmitz, O. J., Wilmers, C. C., Leroux, S. J., Doughty, C. E., Atwood, T. B., Galetti, M., Davies, A. B., & Goetz, S. J. Animals and the zoogeochemistry of the carbon cycle. *Science*, 362, https://doi.org/10.1126/science.aar3213, 2018.

72. Seymour, C. L., Milewski, A. V., Mills, A. J., Joseph, G. S., Cumming, G. S., Cumming, D. H. M. & Mahlangu, Z. Do the large termite mounds of *Macrotermes* concentrate micronutrients in addition to macronutrients in nutrient-poor African savannas? *Soil Biology and Biogeochemistry*, 68, 95-105, https://doi.org/10.1016/j.soilbio.2013.09.022, 2014.

73. Skarpe, C., Aarrestad, P. A., Andreassen, H. P., Dhillion, S. S., Dimakatso, T., du Toit, J. T., Duncan, Halley, J., Hytteborn, H., Makhabu, S., Mari, M., Marokane, W., Masunga, G., Ditshoswane, M., Moe, S. R., Mojaphoko, R., Mosugelo, D., Motsumi, S., Neo-Mahupeleng, G., … Wegge, P. The return of the giants: ecological effects of an increasing elephant population. *Ambio*, 33, 276–282, http://www.jstor.org/stable/4315497, 2004.

74. Sollen-Norrlin, M. & Rintoul-Hynes, N. L. J. Soil sample storage conditions affect measurements of pH, potassium, and nitrogen. *SSSAJ*, 88, 930-941, https://doi.org/10.1002/saj2.20653, 2024.

75. Sonneveld, C. & van den Ende, J. Soil analysis by means of a 1:2 volume extract. Plant and Soil, 63, 523-526, https://www.jstor.org/stable/42933277, 1971.

76. Sterner, R. W., & Elser, J. J. Ecological Stoichiometry: The Biology of Elements from Molecules to the Biosphere. Princeton University Press. http://www.jstor.org/stable/j.ctt1jktrp3, 2002.

77. Subalusky, A. L., Dutton, C. L., Rosi, E. J., & Post, D. M. Annual mass drownings of the Serengeti wildebeest migration influence nutrient cycling and storage in the Mara River. *PNAS*, 114, 7647–7652, https://doi.org/10.1073/pnas.1614778114, 2017.

78. Subalusky, A.L., Dutton, C.L., Rosi, E.J, Puth, L.M., Post, D.M. River of bones: wildebeest skeletons leave a legacy of mass mortality in Mara River, Kenya. *Front. Ecol. Evol.,* 8, https://doi.org/10.3389/fevo.2020.00031, 2020.

79. Towne, E. G. Prairie vegetation and soil nutrient responses to ungulate carcasses. *Oecologia*, 122, 232–239, https://www.jstor.org/stable/4222536, 2000.

80. Turner, B. L. & Romero, T. E. Short-term changes in extractable inorganic nutrients during storage of tropical rainforest soils. *SSSAJ*, 73, 1972-1979, https://doi.org/10.2136/sssaj2008.0407, 2009.

81. Turner, W. C., Kausrud, K. L., Krishnappa, Y. S., Cromsigt, J. P. G. M., Ganz, H. H., Mapaure, I., Cloete, C. C., Havarua, Z., Küsters, M., Getz, W. M., & Stenseth, N. C. Fatal attraction: vegetation responses to nutrient inputs attract herbivores to infectious anthrax carcass sites. *Proc. R. Soc. B*, 281, https://doi.org/10.1098/rspb.2014.1785, 2014.

82. van Klink, R., van Laar-Wiersma, J., Vorst, O., & Smit, C. Rewilding with large herbivores: Positive direct and delayed effects of carrion on plant and arthropod communities. *PloS One*, 15, e0226946, https://doi.org/10.1371/journal.pone.0226946, 2020.

83. Venter, F. J., Scholes, R. J. & Eckhardt, H. C. Abiotic template and its associated vegetation pattern. In: J. T. Du Toit, K. H. Rogers, H. C. Biggs, eds. The Kruger experience: ecology and management of savanna heterogeneity. Washington, DC, USA: Island Press, 83–129, 2003.

749 84. Wiersum, L. K. Uptake of nitrogen and phosphorus in relation to soil structure and nutrient
750 mobility. *Plant Soil,* 16, 62–70, https://doi.org/10.1007/BF01378158, 1962.
751 85. Wigley, B. J., Coetsee, C., Fritz, C. & Bond, W. J. Herbivores shape woody plant
752 communities in the Kruger National Park: lessons from three long-term exclosures: original
753 research. *Koedoe*, 56, http://dx.doi.org/10.4102/koedoe.v56i1.1165, 2014.
754 86. Yang, L. H. Periodical cicadas as resource pulses in North American forests. *Science*, 306,
755 1565–1567, https://doi.org/10.1126/science.1103114, 2004.
756 87. Yang, L. H. Pulses of dead periodical cicadas increase herbivory of American bellflowers.
757 *Ecol.,* 89, 1497–1502, https://doi.org/10.1890/07-1853.1, 2008.
758 88. Yong, S. K., Jalaludin, N. H., Brau, E., Shamsudin, N. N., & Heo, C. C. Changes in soil
759 nutrients (ammonia, phosphate and nitrate) associated with rat carcass decomposition under
760 tropical climatic conditions. *Soil Res*., 57, 482–488, https://doi.org/10.1071/SR18279, 2019.

761 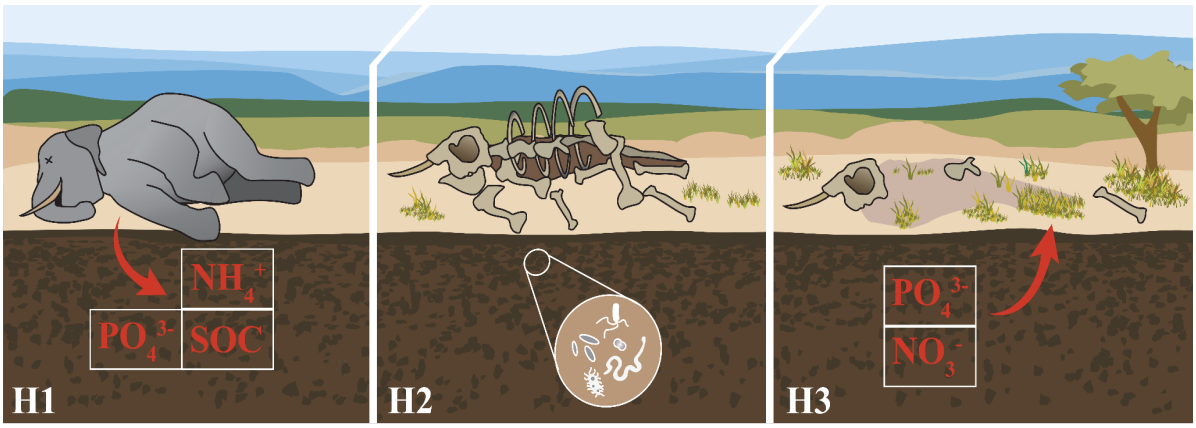

762 **Figure 1.** Hypothesized impacts of elephant megacarcasses on soil and plant nutrients. First
763 (H1), we hypothesized that elephant carcasses would release pulses of nutrients into the soil,
764 resulting in higher concentrations of soil ions such as nitrogen (ammonium, $[NH_4]^+$), phosphorus
765 (phosphate, $[PO_4]^{3-}$), and soil organic C. Second (H2), we hypothesized that C inputs from the
766 carcass would result in increased soil microbial respiration potential. Third (H3), we
767 hypothesized that plants would take up nutrients from the carcass soil, resulting in plants with
768 distinct nutrient profiles and increased concentrations of key limiting nutrients such as N and P.
769 Image credit: Kirsten Boeh.

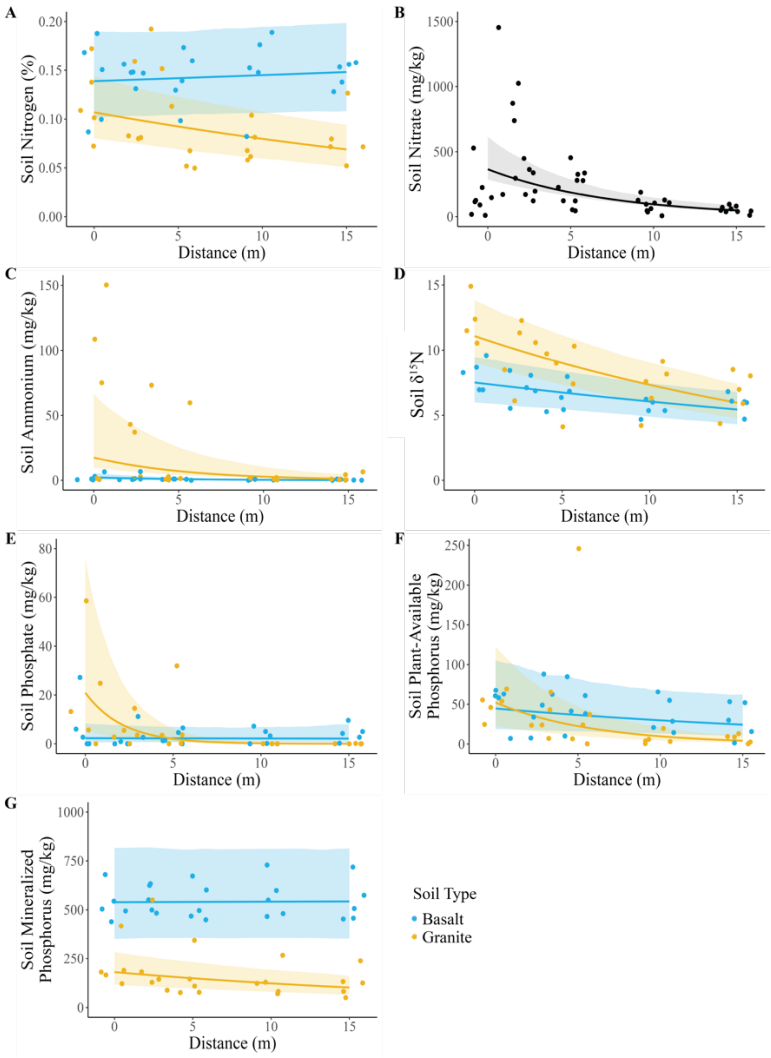

770

771 **Figure 2.** Soil N and P responses to elephant carcasses. (A) Soil N (%) was greater in basaltic
772 soils, and in granitic soils it decreased with distance from the carcass site. (B) Soil nitrate
773 nitrogen decreased with distance but did not differ with soil type. (C) Soil ammonium nitrogen
774 and (D) $\delta^{15}N$ were both greater in granitic soils and decreased with distance from the carcass. (E)
775 Soil phosphate, (F) plant-available P, and (G) mineralized P decreased with distance in granitic
776 soils but not basaltic soils. Points represent individual measurements taken at 0, 2.5, 5, 10, and
777 15m and are offset to be visible when they would otherwise overlap. Lines show predictions
778 calculated from the top model (see Table S1). Shading indicates the 95% confidence interval.

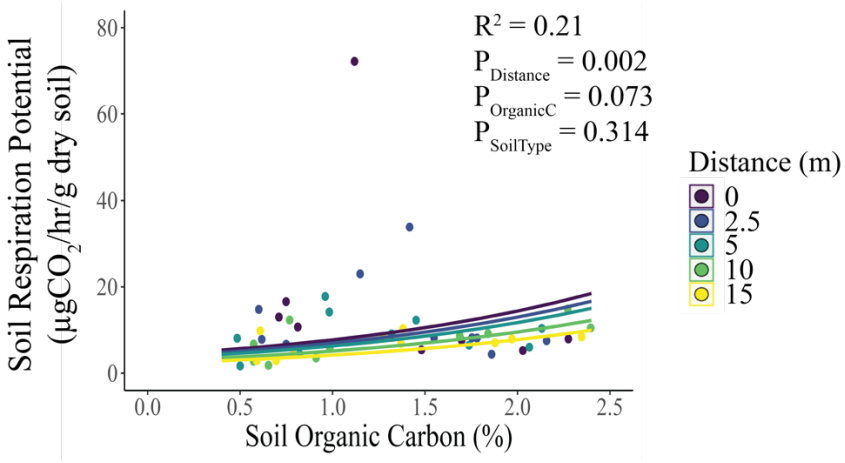

779

780 **Figure 3.** Soil respiration potential was marginally positively correlated with soil organic C (%)

781 and decreased significantly with distance from the carcass. Points represent individual

782 measurements taken at 0, 2.5, 5, 10, and 15m and are offset to be visible when they would

783 otherwise overlap. Lines represent model predictions.

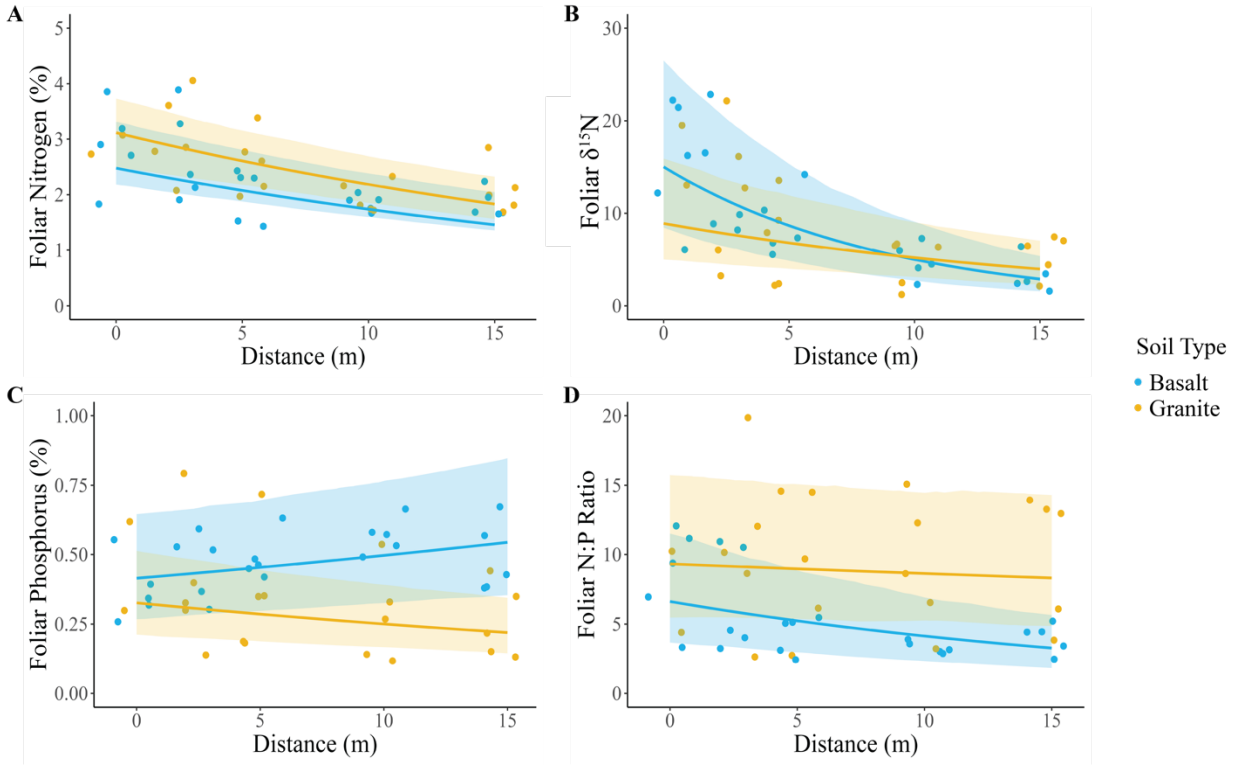

784

785 **Figure 4.** Foliar N and P responses to elephant carcasses. (A) Foliar %N and (B) $\delta^{15}N$ both
786 decreased with distance from the carcass center. (C) Foliar P was greater in basaltic soils and
787 decreased with distance in granitic soils. (D) Foliar N:P ratio was greater in granitic soils and
788 decreased with distance from the carcass center. Points represent individual measurements taken
789 at 0, 2.5, 5, 10, and 15m and are offset to be visible when they would otherwise overlap. Lines
790 show predictions calculated from the top model (see Table S2). Shading indicates the 95%
791 confidence interval. Three of the ten sites had bare ground at the 0 m distance, resulting in a
792 sample size of 7 sites for that distance and 10 for the other distances.

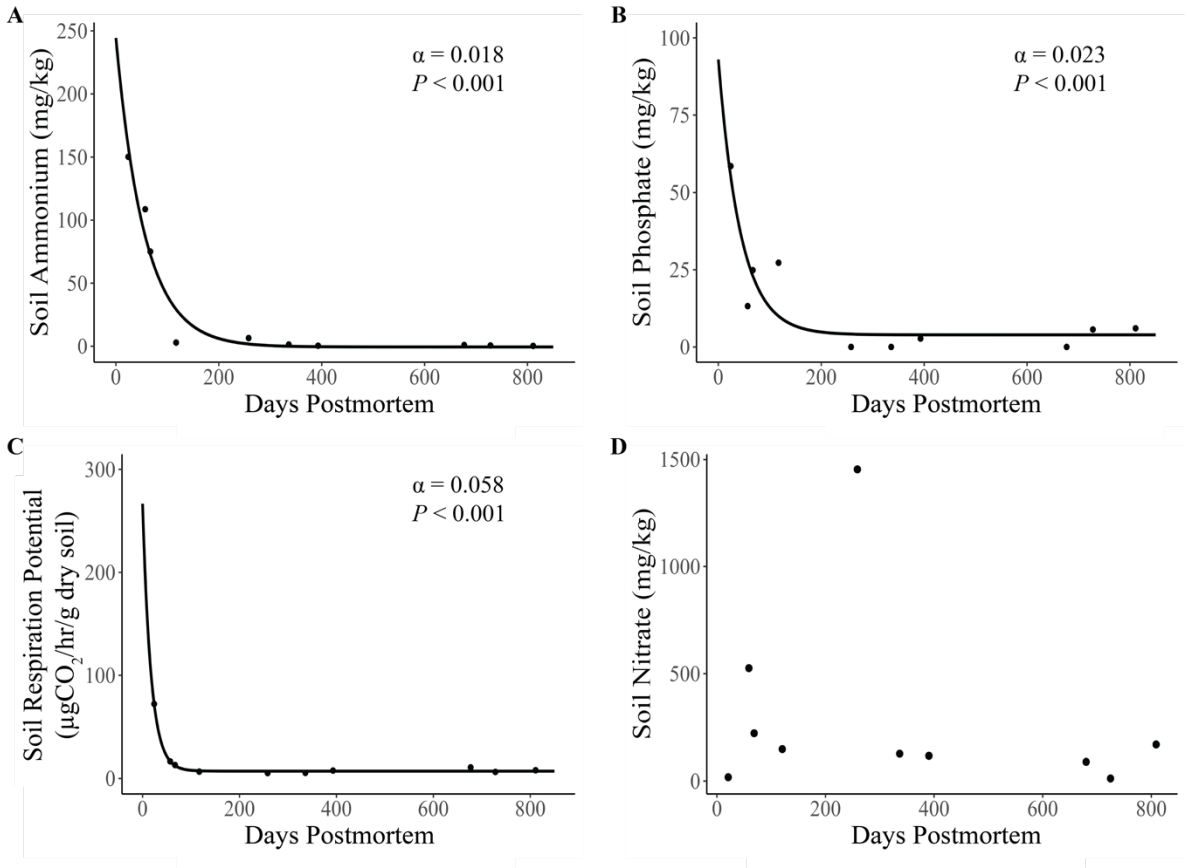

793

794 **Figure 5.** Relationship between carcass age and key soil metrics (soil ion concentrations and
795 respiration potential). Lines represent predictions from exponential decay models, with α equal
796 to the rate of decay. (A) Soil ammonium, (B) phosphate, and (C) respiration potential all
797 decreased significantly with carcass age. The model for (D) soil nitrate failed to converge. Points
798 represent individual measurements taken at the center of the carcass site (distance = 0.5m).